

# <sup>1</sup> KIM: Knowledge-Informed Mapping (KIM) Toolkit

<sup>2</sup> Peishi Jiang  <sup>1,2</sup>, Aaron Wang<sup>1</sup>, Susannah M. Burrows<sup>1</sup>, Naser Mahfouz<sup>1</sup>,  
<sup>3</sup> and Xingyuan Chen<sup>1</sup>

<sup>4</sup> 1 Atmospheric, Climate, and Earth Sciences Division, Pacific Northwest National Laboratory, Richland,  
<sup>5</sup> Washington, USA 2 Civil, Construction and Environmental Engineering, University of Alabama,  
<sup>6</sup> Tuscaloosa, Alabama, USA

DOI: [10.xxxxxx/draft](https://doi.org/10.xxxxxx/draft)

## Software

- [Review](#) 
- [Repository](#) 
- [Archive](#) 

<sup>7</sup> Peishi Jiang<sup>1,2</sup>, Aaron Wang<sup>1</sup>, Susannah M. Burrows<sup>1</sup>, Naser Mahfouz<sup>1</sup>, Xingyuan Chen<sup>1</sup>

<sup>8</sup> 1 Atmospheric, Climate, and Earth Sciences Division, Pacific Northwest National Laboratory,  
<sup>9</sup> Richland, WA, USA

<sup>10</sup> 2 Civil, Construction and Environmental Engineering, University of Alabama, Tuscaloosa, AL,  
<sup>11</sup> USA

Editor: Vangelis Kourlitis  

Submitted: 21 August 2025

Published: unpublished

## License

Authors of papers retain copyright and release the work under a Creative Commons Attribution 4.0 International License ([CC BY 4.0](#)). We expect this toolkit will be helpful to glue the model data integration for Earth science applications.

## <sup>12</sup> Summary

We present a Knowledge-Informed Mapping toolkit in Python programming language, named KIM, to optimize the development of the mapping from a vector of inputs  $\mathbf{X}$  to a vector of outputs  $\mathbf{Y}$ . KIM builds on the methodology development of deep learning-based inverse mapping in Jiang et al. (2023) and A. Wang et al. (2025). KIM offers a preliminary understanding of data interdependencies while optimizing the training step with uncertainty accounted for. We expect this toolkit will be helpful to glue the model data integration for Earth science applications.

## <sup>20</sup> Statement of need

Striving for scientific hypothesis testing and discovery, Earth scientists oftentimes develop data-driven mappings – either for inverse modeling, as part of model calibration, or forward modeling, as an emulator. Both approaches benefit from an efficient way of mapping, , that projects from a vector of inputs  $\mathbf{X}$  to a vector of outputs  $\mathbf{Y}$ . Such mapping approach has seen successes in addressing inverse and forward problems in multiple studies across Earth sciences (Cromwell et al., 2021; HU et al., 2014; Krasnopolksy & Schiller, 2003; Mudunuru et al., 2022).

Nevertheless, constructing the mapping that connects all inputs  $\mathbf{X}$  to all outputs  $\mathbf{Y}$  is usually challenging due to (1) limited data/simulations for training; (2) uninformative relations between some members of  $\mathbf{X}$  and  $\mathbf{Y}$ ; and (3) the structural uncertainty of the mapping . To that, Jiang et al. (2023) and A. Wang et al. (2025) leveraged the idea of integrating scientific knowledge with deep learning (Willard et al., 2022) to develop knowledge-informed mapping (KIM). The goal of this paper is to document and open source KIM for a general public usage. Figure 1 shows the general procedures of KIM which are detailed in the next section.

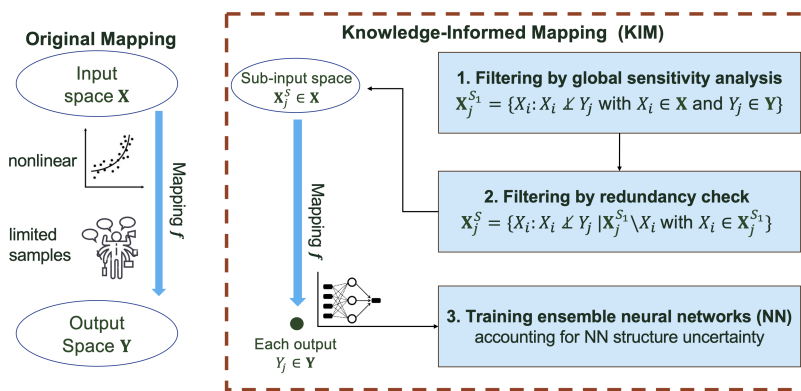


Figure 1: Comparison between KIM and the original mapping.

## 35 Mathematical approach

36 Consider a vector of inputs  $\mathbf{X} = [X_1, \dots, X_{N_x}]$  and a vector of outputs  $\mathbf{Y} = [Y_1, \dots, Y_{N_y}]$ . The  
 37 objective is to build up a mapping function  $f$  from  $\mathbf{X}$  to  $\mathbf{Y}$ , such that  $f : \mathbb{R}^{N_x} \rightarrow \mathbb{R}^{N_y}$ , based  
 38 on  $N_e$  pairs/realizations of  $\mathbf{X}$  and  $\mathbf{Y}$ . Instead of developing a lumped mapping, we aim to  
 39 develop a separate inverse mapping  $f_i$  for each  $Y_j \in \mathbf{Y}$  by using a reduced space  $\mathbf{X}_j^S \in \mathbf{X}$   
 40 that is most relevant to  $Y_j$ , such that  $f_j : \mathbb{R}^{N_{x_j}} \rightarrow \mathbb{R}$  (see examples in Jiang et al. (2023) and  
 41 A. Wang et al. (2025)), which involves the following steps.

42 **Step 1: Filtering by global sensitivity analysis.** We first perform a mutual information-based  
 43 global sensitivity analysis to narrow down a subset  $\mathbf{X}_j^{S_1}$ , each of which shares zero information  
 44 with  $Y_j$  such that:

$$\mathbf{X}_j^{S_1} = \{X_i : I(X_i; Y_j) \neq 0 \text{ with } X_i \in \mathbf{X}\},$$

45 where  $I(X_i; Y_j)$  is the mutual information between  $X_i$  and  $Y_j$  (Cover & Thomas, 2006). Based  
 46 on the  $N_e$  realizations,  $I$  is calculated on the joint probability of  $X_i$  and  $Y_j$  using either binning  
 47 method or k-nearest-neighbor method.

48 **Step 2: Filtering by redundancy check.** Then, we conduct a further assessment that filters out  
 49 any model output in  $\mathbf{X}_j^{S_1}$  whose dynamics are redundant to  $Y_j$  given the knowledge of other  
 50 outputs. This is achieved through a conditional independence test using conditional mutual  
 51 information (Cover & Thomas, 2006) given as:

$$\mathbf{X}_j^S = \{X_i : I(X_i; Y_j | \mathbf{X}_j^{S_1} \setminus X_i) \neq 0 \text{ with } X_i \in \mathbf{X}_j^{S_1}\},$$

52 where  $\mathbf{X}_j^{S_1} \setminus X_i$  is the remaining set of  $\mathbf{X}_j^{S_1}$  by excluding  $X_i$ ;  $I(X_i; Y_j | \mathbf{X}_j^{S_1} \setminus X_i)$  is the con-  
 53 ditional mutual information between  $X_i$  and  $Y_j$  conditioning on  $\mathbf{X}_j^{S_1} \setminus X_i$ .  $I(X_i; Y_j | \mathbf{X}_j^{S_1} \setminus X_i) = 0$   
 54 indicates that  $X_i$  and  $Y_j$  are independent given the knowledge of  $\mathbf{X}_j^{S_1} \setminus X_i$ .

55 **Step 3: Uncertainty aware estimation by training ensemble neural networks.** For each parameter  
 56  $Y_i$ , we train an ensemble of fully-connected neural networks by varying the hyperparameters,  
 57 including the number of hidden layers, the number of hidden neurons, and the learning rate. We  
 58 split the  $N_e$  model realizations into training, validation, and testing dataset. When evaluating  
 59 the estimation on the test dataset, we further quantified the bias and uncertainty of the

60 prediction as:

$$\text{Bias} = E(|\mu_w - y|)$$
$$\text{Uncertainty} = E(\sigma_w / |y|),$$

61 where  $E$  is the expectation operator;  $y$  is the true value;  $\mu_w$  and  $\sigma_w$  are the mean and standard  
62 deviation of the ensemble predictions weighted by their accuracy in the validation set.

## 63 Examples

64 We present two applications of KIM in performing inverse modeling, with Jupyter notebook  
65 provided in the repository to guide the package usage. For each case, we developed three types  
66 of inverse mappings: (1) the original inverse mapping without knowledge-informed, denoted as  
67  $M_0$ ; (2) the knowledge-informed inverse mapping only using global sensitivity analysis (Step  
68 1), denoted as  $M_1$ ; and (3) the knowledge-informed inverse mapping using both Step 1 and  
69 Step 2, denoted as  $M_2$ . The configurations can be found in the example jupyter notebook.

70 **Case 1: Calibrating a cloud chamber model.** Cloud chamber model has been widely applied  
71 as a virtual reality of a true cloud chamber to study turbulence, clouds, and their interactions  
72 (Thomas et al., 2019; Aaron Wang, Ovchinnikov, Yang, Schmalfuss, et al., 2024; Aaron Wang,  
73 Ovchinnikov, Yang, Cantrell, et al., 2024; Aaron Wang, Krueger, et al., 2024; Aaron Wang et  
74 al., 2025). The objective of this example is to estimate two key parameters, i.e., the scaling  
75 coefficients of wall fluxes ( $\lambda_w$ ) and collision processes ( $\lambda_c$ ) using inverse mapping. To that,  
76 an ensemble of 513 model runs were generated based on a model set up detailed in A. Wang  
77 et al. (2025), by varying the values of the two parameters using Sobol sequence. 27 virtual  
78 sensors are configured, each of which 'records' multiple variables including flow properties and  
79 cloud properties.

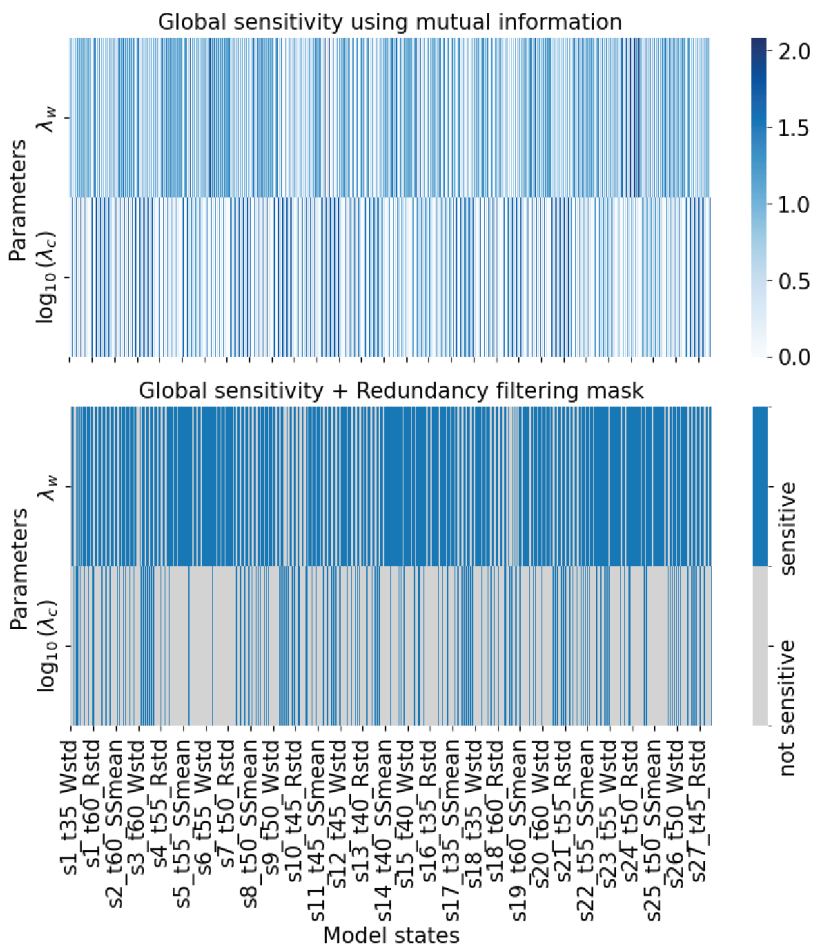


**Figure 2:** Preliminary analysis of cloud chamber ensemble modeling.

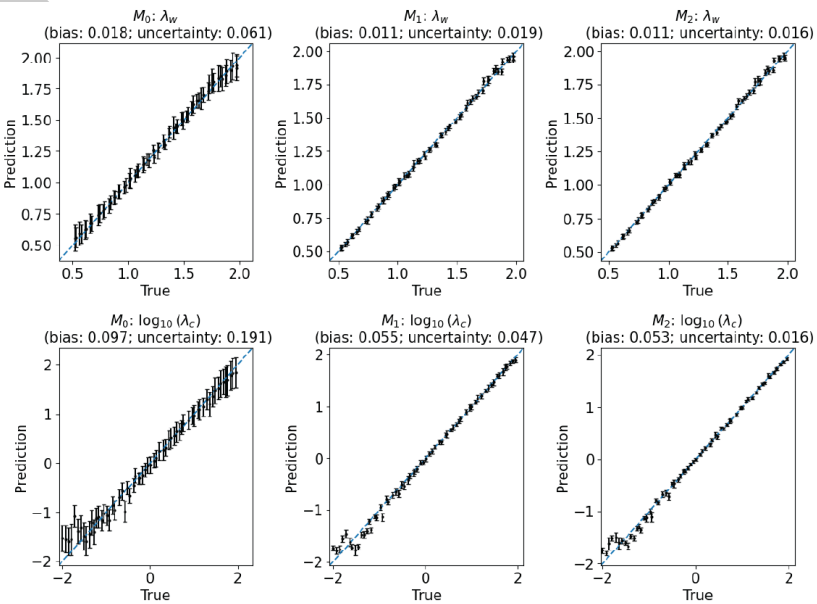


**Figure 3:** Parameter estimation of the cloud chamber model.

80   **Case 2: Calibrating an integrated hydrological model.** The Advanced Terrestrial Simulator  
 81 (ATS) is an integrated hydrological models used to simulate hydrological fluxes across a  
 82 watershed ([Coon et al., 2019](#)). Here, we calibrated ATS against the streamflow observations  
 83 at the outlet of Coal Creek watershed, CO, USA. The objective is to estimate eight models  
 84 parameters categorized into evapotranspiration (ET), snow melting, and subsurface permeability.  
 85 See [Jiang et al. \(2023\)](#) for more detailed information.

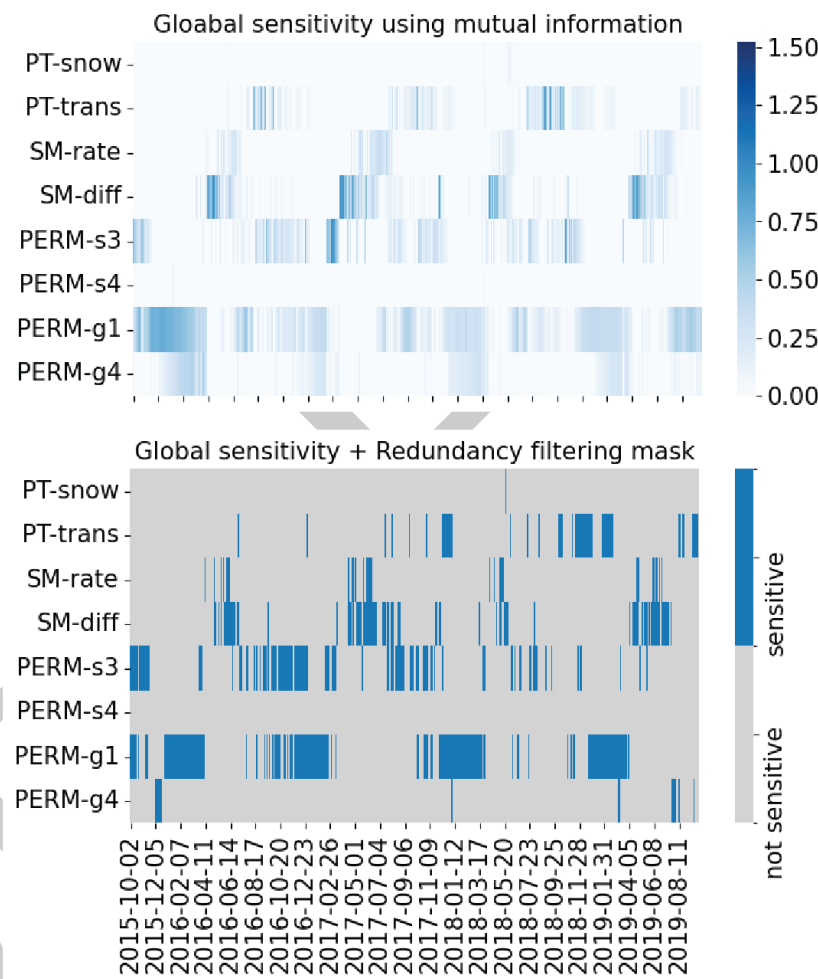


**Figure 4:** Preliminary analysis of ATS ensemble modeling.

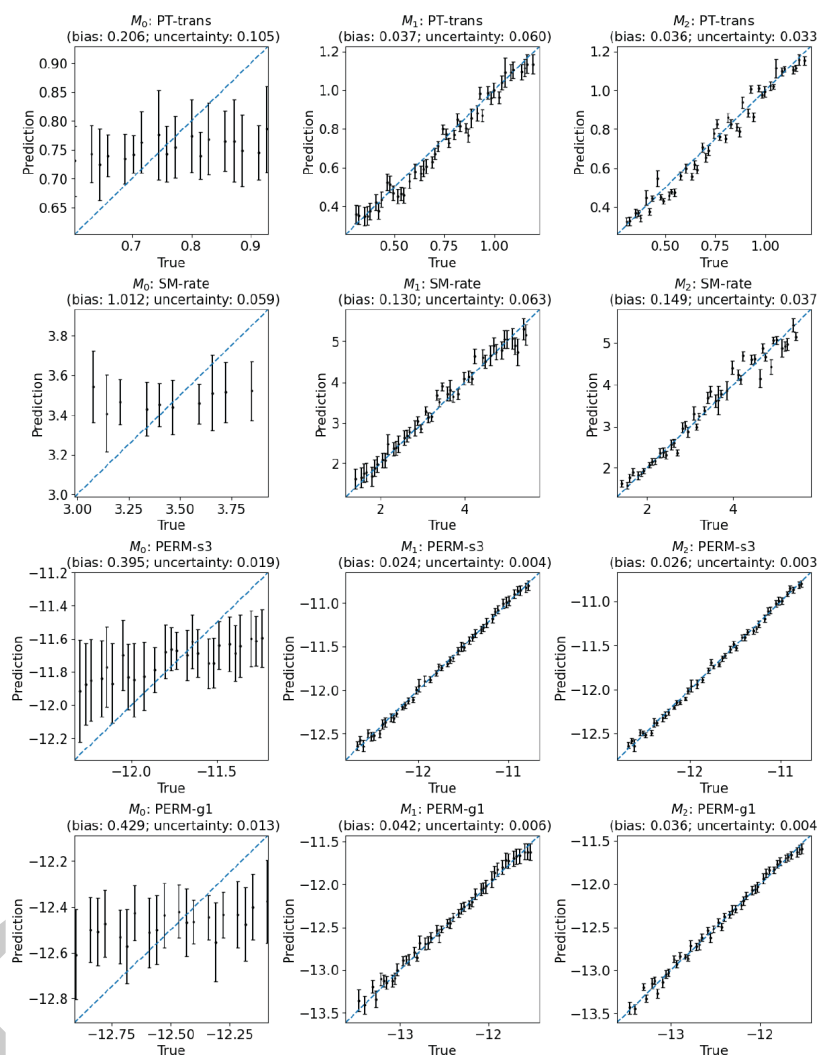


Figure 5: Parameter estimation of the ATS model.

## 86 Acknowledgements

87 This work was supported by both the Laboratory Directed Research and Development Program  
 88 at Pacific Northwest National Laboratory and the IDEAS-Watersheds project. The Laboratory  
 89 Directed Research and Development Program at Pacific Northwest National Laboratory is a  
 90 multiprogram national laboratory operated by Battelle for the U.S. Department of Energy.  
 91 Pacific Northwest National Laboratory is operated for the DOE by Battelle Memorial Institute  
 92 under contract DE-AC05-76RL01830. The IDEAS-Watersheds project is funded by the U.S.  
 93 Department of Energy (DOE), Office of Science (SC) Biological and Environmental Research  
 94 (BER) program, as part of BER's Environmental System Science (ESS) program.

## 95 References

- 96 Coon, E., Svyatsky, D., Jan, A., Kikinzon, E., Berndt, M., Atchley, A., Harp, D., Manzini,  
 97 G., Shelef, E., Lipnikov, K., Garimella, R., Xu, C., Moulton, D., Karra, S., Painter, S.,  
 98 Jafarov, E., & Molins, S. (2019). *Advanced terrestrial simulator*. [Computer Software]  
<https://doi.org/10.11578/dc.20190911.1> <https://doi.org/10.11578/dc.20190911.1>

- 100 Cover, T. M., & Thomas, J. A. (2006). *Elements of information theory (wiley series in*  
101 *telecommunications and signal processing)*. Wiley-Interscience. ISBN: 0471241954
- 102 Cromwell, E., Shuai, P., Jiang, P., Coon, E. T., Painter, S. L., Moulton, J. D., Lin, Y., &  
103 Chen, X. (2021). Estimating watershed subsurface permeability from stream discharge  
104 data using deep neural networks. *Frontiers in Earth Science*, 9. <https://doi.org/10.3389/feart.2021.613011>
- 105 HU, Y., YU, X., LI, S., CHEN, G., ZHOU, Y., & GAO, Z. (2014). Improving the accuracy of  
106 geological model by using seismic forward and inverse techniques. *Petroleum Exploration and*  
107 *Development*, 41(2), 208–216. [https://doi.org/https://doi.org/10.1016/S1876-3804\(14\)60024-0](https://doi.org/10.1016/S1876-3804(14)60024-0)
- 108 Jiang, P., Shuai, P., Sun, A., Mudunuru, M. K., & Chen, X. (2023). Knowledge-informed  
109 deep learning for hydrological model calibration: An application to coal creek watershed in  
110 colorado. *Hydrology and Earth System Sciences*, 27(14), 2621–2644. <https://doi.org/10.5194/hess-27-2621-2023>
- 111 Krasnopolsky, V. M., & Schiller, H. (2003). Some neural network applications in envi-  
112 ronmental sciences. Part i: Forward and inverse problems in geophysical remote mea-  
113 surements. *Neural Networks*, 16(3), 321–334. [https://doi.org/https://doi.org/10.1016/S0893-6080\(03\)00027-3](https://doi.org/https://doi.org/10.1016/S0893-6080(03)00027-3)
- 114 Mudunuru, M. K., Son, K., Jiang, P., Hammond, G., & Chen, X. (2022). Scalable deep  
115 learning for watershed model calibration. *Frontiers in Earth Science, Volume 10 - 2022.*  
116 <https://doi.org/10.3389/feart.2022.1026479>
- 117 Thomas, S., Ovchinnikov, M., Yang, F., Voort, D. van der, Cantrell, W., Krueger, S. K., &  
118 Shaw, R. A. (2019). Scaling of an atmospheric model to simulate turbulence and cloud  
119 microphysics in the pi chamber. *Journal of Advances in Modeling Earth Systems*, 11(7),  
120 1981–1994.
- 121 Wang, A., Jiang, P., Burrows, S., Glienke, S., Ovchinnikov, M., & Mahfouz, N. (2025). *Inverse*  
122 *mapping of the collision kernel and wall flux scaling in a large-scale convection-cloud*  
123 *chamber using local sensors and knowledge-informed deep learning.*
- 124 Wang, Aaron, Krueger, S., Chen, S., Ovchinnikov, M., Cantrell, W., & Shaw, R. A. (2024).  
125 Glaciation of mixed-phase clouds: Insights from bulk model and bin-microphysics large-eddy  
126 simulation informed by laboratory experiment. *Atmospheric Chemistry and Physics*, 24(18),  
127 10245–10260.
- 128 Wang, Aaron, Ovchinnikov, M., Yang, F., Cantrell, W., Yeom, J., & Shaw, R. A. (2024). The  
129 dual nature of entrainment-mixing signatures revealed through large-eddy simulations of a  
130 convection-cloud chamber. *Journal of the Atmospheric Sciences*, 81(12), 2017–2039.
- 131 Wang, Aaron, Ovchinnikov, M., Yang, F., Schmalfuss, S., & Shaw, R. A. (2024). Designing a  
132 convection-cloud chamber for collision-coalescence using large-eddy simulation with bin  
133 microphysics. *Journal of Advances in Modeling Earth Systems*, 16(1), e2023MS003734.
- 134 Wang, Aaron, Schmalfuß, S., Chandrakar, K. K., Kia, H. Z., Yang, F., Ovchinnikov, M.,  
135 Shaw, R. A., & Choi, Y. (2025). An intercomparison of wall fluxes in a turbulent thermal  
136 convection chamber: Direct numerical simulations and wall-modeled large-eddy simulations  
137 enhanced by machine learning. *Physics of Fluids*, 37(4).
- 138 Willard, J., Jia, X., Xu, S., Steinbach, M., & Kumar, V. (2022). Integrating scientific knowledge  
139 with machine learning for engineering and environmental systems. *ACM Comput. Surv.*,  
140 55(4). <https://doi.org/10.1145/3514228>
- 141